Morphology control of poly(methyl methacrylate) particles via seeded dispersion polymerization

Morishita, Takahiro
Ikeda, Hayate
Suzuki, Nozomu
Suzuki, Toyoko
Minami, Hideto

(Citation)
Next Materials,10:101432

(Issue Date)
2026-01

(Resource Type)
journal article

(Version)
Version of Record

Next Materials 10 (2026) 101432

Contents lists available at ScienceDirect

Next Materials

journal homepage: www.sciencedirect.com/journal/next-materials

Morphology control of poly(methyl methacrylate) particles via seeded dispersion polymerization

Takahiro Morishita, Hayate Ikeda, Nozomu Suzuki, Toyoko Suzuki, Hideto Minami [1,*]

Department of Chemical Science and Engineering, Graduate School of Engineering, Kobe University, 1-1 Rokko, Nada-ku, Kobe 657-8501, Japan

ARTICLE INFO

Keywords:
Nonspherical particle
Polymer
Seeded dispersion polymerization
Glass transition temperature
Hansen solubility parameters

ABSTRACT

Nonspherical polymer particles have been studied for several decades because their properties, such as mechanical and optical properties, differ from those of spherical particles. Their potential in advanced applications has continued to drive interest in developing shape-controlled synthesis methods. In this study, we investigated the shape control of poly(methyl methacrylate) (PMMA) particles during seeded dispersion polymerization (SDP) of styrene using PMMA as seed particles in the presence of various hydrocarbons. By systematically varying the polymerization temperature (T_r) and hydrocarbon type, we successfully fabricated PMMA particles with diverse morphologies, specifically golf ball-like, bowl-like, and barrel-like structures. Results revealed that the difference between T_r and the glass transition temperature (T_g) of the seed particles (T_r–T_g) plays a critical role in determining the particle shape. Furthermore, an index was formulated based on Hansen solubility parameters to quantify the affinity differences between the seed and second polymers for the medium, which helped explain the behavior of the second polymer domain during polymerization. The use of a hydrophilic initiator suppressed the submergence of domains into the seed particle, facilitating the formation of polyhedral and disk-like particles. This paper contributes to the development of a generalized strategy for the synthesis of shape-controlled nonspherical polymer particles via SDP.

1. Introduction

Polymer particles produced using heterogeneous systems, such as dispersion polymerization and emulsion polymerization systems, generally adopt spherical morphologies to minimize the interfacial free energy between the particles and the surrounding media. While spherical particles can be produced using relatively simple methods, they do not always satisfy the functional requirements of advanced applications. Consequently, nonspherical particles have been extensively studied for decades due to their unique physical properties [1–3]. Their utilities as functional materials have been recognized in various applications, including coatings [4], cosmetics [5], light-scattering agents [6], and catalyst support [7–9]. The physical properties of nonspherical particles differ from those of spherical particles in terms of mechanical and fluid dynamic characteristics, prompting extensive research on their synthesis methods over the years [10,11].

Several approaches have been developed to fabricate such nonspherical particles, including techniques based on microfluidics [12] and the application of mechanical stress [13–15]. Okubo et al. prepared diverse nonspherical particles, such as those with golf ball-, tetrapod- and disk-like morphologies, through seeded dispersion polymerization (SDP) of 2-ethylhexyl methacrylate (EHMA) in the presence of hydrocarbons using polystyrene (PS) particles as seeds [16,17]. Furthermore, Qiao et al. successfully controlled the shape of disc-like particles through SDP of EHMA in the presence of decane using PS particles with shells of varying degrees of hydrophilicity as seeds [18]. SDP is advantageous because it enables the formation of thermodynamically unstable structures whose morphologies can be controlled by varying their polymerization conditions. They have also formed golf ball-like particles using poly(methyl methacrylate) (PMMA), a widely used general-purpose polymer, as seeds in SDP [19]. Additionally, Asua et al. prepared nonspherical hybrid polymer particles composed of PMMA and PS via seeded emulsion polymerization using PMMA particles as seeds [20,21]. These studies demonstrate that seeded polymerization can be an effective strategy for morphology control even in relatively polar, general-purpose polymers such as PMMA, providing valuable insights into particle shape design. However, the shape control of PMMA-based particles remains underexplored.

* Corresponding author.
E-mail address: minamihi@kobe-u.ac.jp (H. Minami).
[1] ORCID: orcid.org/0000–0001-6173–6597

https://doi.org/10.1016/j.nxmate.2025.101432
Received 9 July 2025; Received in revised form 25 October 2025; Accepted 11 November 2025
Available online 19 November 2025

In this study, to expand SDP applicability to various type of polymer particles for producing varioiu shape of nonspherical particles, we aim to fabricate nonspherical particles through SDP of styrene using PMMA particles as seeds in the presence of hydrocarbons. We achieve various particle shapes by modulating the polymerization parameters, specifically the hydrocarbon type and the reaction temperature (T_r) (= the polymerization temperature). Furthermore, by investigating the relationship between the polymerization conditions and the obtained particle morphologies, we elucidate the key factors governing shape formation in SDP as compared with PS seed system.

2. Experimental section

2.1. Materials

Methyl methacrylate (MMA) and styrene were obtained from Nacalai Tesque Inc. (Kyoto, Japan); they were purified via distillation under reduced pressure in a N_2 atmosphere. The initiator 2,2′-azobis(isobutyronitrile) (AIBN; Fujifilm Wako Pure Chemical Co., Osaka, Japan) was purified in methanol via recrystallization. Hexadecane, decahydronaphthalene (decalin), tetralin, cyclohexanol, chlorobenzene, tetrahydrofuran (THF), acetone, acetic anhydride, N-methyl-2-pyrrolidone, N,N-dimethylformamide (DMF), dimethyl sulfoxide (DMSO), acetonitrile, 1-pentanol, 1-butanol, ethanol, methanol, poly(vinylpyrrolidone) (PVP, K-30: $M_w = 4.0 \times 104$), and polyethylene glycol (PEG-OH: $M_w = 2.0 \times 103$) were obtained from Nacalai Tesque Inc. (Kyoto, Japan) and used as received. Hexane, toluene, VPE-0201, and 2,2′-azobis(4-methoxy-2,4-dimethylvaleronitrile) (V-70) were obtained from Fujifilm Wako Pure Chemical Co. (Osaka, Japan) and used as received. Phenylcyclohexane, m-cresol, and indan were obtained from Tokyo Chemical Industry Co. (Tokyo, Japan) and used as received. Acetic acid, 1,4-dioxane, and 2-propanol were obtained from Junsei Chemical Co. Ltd. (Tokyo, Japan) and used as received. Ruthenium tetraoxide (RuO_4) was obtained from Filgen Inc. (Aichi, Japan) and used as received. The utilized water was purified using an ErixUV purification system (Merck Millipore, Tokyo, Japan; resistivity, >5 MΩ cm).

2.2. Preparation of PMMA particles via dispersion polymerization

MMA (65 g), PVP (K-30, 15 g), and AIBN (1.3 g) were dissolved in a mixture of methanol (455 g) and water (195 g). This solution was poured into a separate flask (1000 mL) and stirred at 300 rpm (mechanical stirrer) in a water bath at 65°C for 24 h in a N_2 atmosphere. The obtained PVP-stabilized PMMA particles were washed with methanol, and the medium was replaced with methanol via centrifugation.

2.3. Preparation of nonspherical particles via seeded dispersion polymerization of styrene

The typical SDP procedure was performed as follows: styrene (0.125 g), AIBN (3 mg), and PVP (K-30, 50 mg) were dissolved in a mixture of methanol (8 g) and water (2 g), and this solution was poured into a Schlenk flask (25 mL). The PMMA seed particles (0.25 g) and decalin droplets (1.25 g) were also dispersed in the solution. The resulting mixture was stirred at 400 rpm (magnetic stirrer) in a water bath at 65°C for 24 h in a N_2 atmosphere. After polymerization, the obtained particles were washed with methanol via centrifugation to remove hydrocarbons.

We controlled the particle morphology by modifying the hydrocarbon (decalin, tetralin, or indan), T_r (between 40°C and 70°C), and the hydrophilicity of the second polymer using an initiator (AIBN–VPE-0201).

2.4. Measurement of glass transition temperature via differential scanning calorimetry (DSC)

The PMMA seed particles were dried in a vacuum. The glass transition temperature (T_g) was measured using approximately 5 mg of the dried PMMA particles or the PMMA particles soaked in different hydrocarbons (decalin, indan, or tetralin) through DSC (7000X, Hitachi High-Tech Science Co., Japan) at −40°C to 130°C at 5 °C/min under a N_2 flow. Heating and cooling operations were each performed three times, and the evaluation used data from the second heating cycle.

2.5. Hansen dissolution tests for polymers

Hansen solubility/dissolution tests were conducted for the three polymers, PMMA pellet, PS pellet, and poly(2-ethylhexyl methacrylate) (PEHMA) prepared via bulk polymerization. Each polymer pellet was mixed with each tested solvent (hexane, hexadecane, decalin, phenylcyclohexane, toluene, 1,4-dioxane, tetralin, cyclohexanol, chlorobenzene, THF, m-cresol, acetic acid, pyridine, acetone, acetic anhydride, N-methyl-2-pyrrolidone, DMF, DMSO, acetonitrile, 1-pentanol, 1-butanol, 2-propanol, ethanol, methanol, and water), and the resulting mixtures were continuously stirred at room temperature overnight. The solubility of the polymers in each solvent was visually checked and recorded in the software HSPiP (Pirika, Japan) to prepare Hansen spheres. The center coordinate of each sphere was defined as the Hansen solubility parameter (HSP) of the corresponding polymer. The HSPs for the solvents and hydrocarbons were obtained from the software.

2.6. Characterization

The obtained particles were analyzed through optical microscopy (ECLIPSE 80i, Nikon Corporation, Tokyo, Japan) and scanning electron microscopy (SEM; JSM-6510, JEOL, Tokyo, Japan; at 20 kV). The number-average diameter (D_n) and coefficient of variation (C_V) were determined by counting over 100 particles using the image analysis software WinROOF (Mitani Co., Fukui, Japan). The interior morphology of the nonspherical particles was analyzed using ultrathin sections (thickness: 100 nm) obtained using an EM UC6 microtome with an EM FC7 cryochamber (Leica, Tokyo, Japan). In microtomy, the dried particles were stained with RuO_4 vapor at room temperature for 30 min in the presence of a RuO_4 crystal and embedded with epoxy-matrix and kept overnight at room temperature. Next, the ultrathin cross sections were observed via transmission electron microscopy (TEM; JEM-1230, JEOL, Tokyo, Japan; at 100 kV).

3. Results and discussion

Micron-sized monodisperse PMMA particles were prepared via dispersion polymerization using PVP as the dispersion stabilizer (Fig. 1). The obtained PMMA particles were spherical and monodisperse, with D_n and C_V values of 1.9 μm and 3.8 %, respectively. Subsequently, the nonspherical PMMA particles were prepared through SDP of styrene in the presence of the hydrocarbon droplets and the PMMA seed particles. The SDP mechanism in the presence of hydrocarbons was as follows (Scheme 1). The second monomer was dissolved in the medium, which contained hydrocarbon droplets. The polymer obtained through the polymerization of the second monomer had a higher affinity for the seed polymer than the medium, precipitating the second polymer on the seed particle. As the hydrocarbon exhibited a higher affinity for the second polymer than the seed polymer, it was predominantly absorbed in the precipitated second polymer, forming domains on the seed particle. The domains remained separate on the seed particle surface at a sufficiently high viscosity of the seed particle, thereby forming a golf ball-like particle. At a low viscosity of the seed particle, the domains migrated and coalesced on the seed particle surface, forming bowl-, barrel-, or disk-like particles. After polymerization, the hydrocarbon was removed,

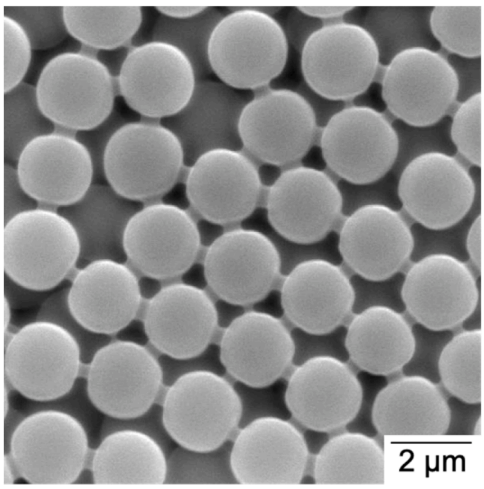

Fig. 1. SEM image of PMMA seed particles prepared via dispersion polymerization.

allowing for the formation of indentations on the particle surface, where the second polymer remained. Considering the considerable effect of the viscosity of the seed particles on the preparation of the nonspherical particles, we investigated the possible effects of varying the temperature difference relative to the T_g of the seed particles by changing the T_r. Here, decalin was used as the hydrocarbon, as it had a higher affinity for PS than PMMA in terms of the HSP distance (Table 1).

The nonspherical particles were prepared through SDP of styrene in a methanol–water (80/20, w/w) medium in the presence of decalin droplets and PMMA seed particles at 40°C–70°C. The particles were washed with methanol to remove the hydrocarbon, which is a poor solvent for PMMA and PS.

Fig. 2 shows the optical microscope and SEM images of the obtained PMMA/PS particles. At T_r of 40°C (Figure S1, SEM and TEM), 50°C (a, a'), and 60°C (b, b'), the observed particles have a golf ball-like structure. This was because the relatively high viscosity of the seed particle suppressed the migration and coalescence of the domains that formed on it. Note that V-70 was used for the reaction at 40°C instead of AIBN, given the low decomposition rate of AIBN at 40°C. Bowl- and barrel-like particles were obtained at T_r of 65°C (c, c') and 70°C (d, d') due to the low viscosity of the seed particle, which caused the formation, migration, and coalescence of domains on its surface. Furthermore, the low affinity of the PS–decalin domains for the medium caused the domains to be submerged inside the seed particle. In addition, particle deformation did not occur when polymerization was carried out at 65°C without styrene or decalin (Figure S2, S3). This confirmed that both the second monomer and the hydrocarbon were essential for particle deformation, as shown in Scheme 1. Based on the formation mechanism of nonspherical particles via SDP (Scheme 1), nonspherical particles can also be obtained by selectively extracting the second polymer phase using an appropriate solvent, while retaining their original morphology essentially [22]. Here, the significant change in the particle shape after a slight temperature shift from 60°C to 65°C suggested that the seed particle viscosity rapidly decreased at approximately 65°C.

We confirmed the change in the T_g of PMMA in the presence of the hydrocarbon by performing DSC measurement on PMMA particles (dry state and soaked in decalin), resulting in T_g values without and with decalin at 112°C and 65°C, respectively (Fig. 3). The results indicated that decalin did not dissolve the PMMA particles but swelled and plasticized them, reducing their viscosity near the lowered T_g. Therefore, the decrease in viscosity of the seed polymer, PMMA, caused the golf ball-like particles to transform into bowl-like particles.

The particle shape change caused by the T_g decrease of PMMA was further examined by changing the hydrocarbon into tetralin and indan during SDP of styrene at 65°C in a methanol–water (80/20, w/w) medium. Tetralin and indan are poor-solvent, however, they were expected to have a higher affinity for PMMA than decalin from the viewpont of

Table 1
Measured HSPs of PMMA, PS, and hydrocarbons and HSP distances between each polymer and each hydrocarbon.

	δD	δP	δH	HSP distance	
	(Dispersion)	(Polarity)	(Hydrogen-bond)	vs PMMA	vs PS
PMMA	16.9	10	6.5		
PS	17.6	7.5	4.8		
Decalin	17.8	0	0	12.06	8.91
Tetralin	19.6	2	2.9	10.3	7.06
Indan	19	3	2.9	8.92	5.63

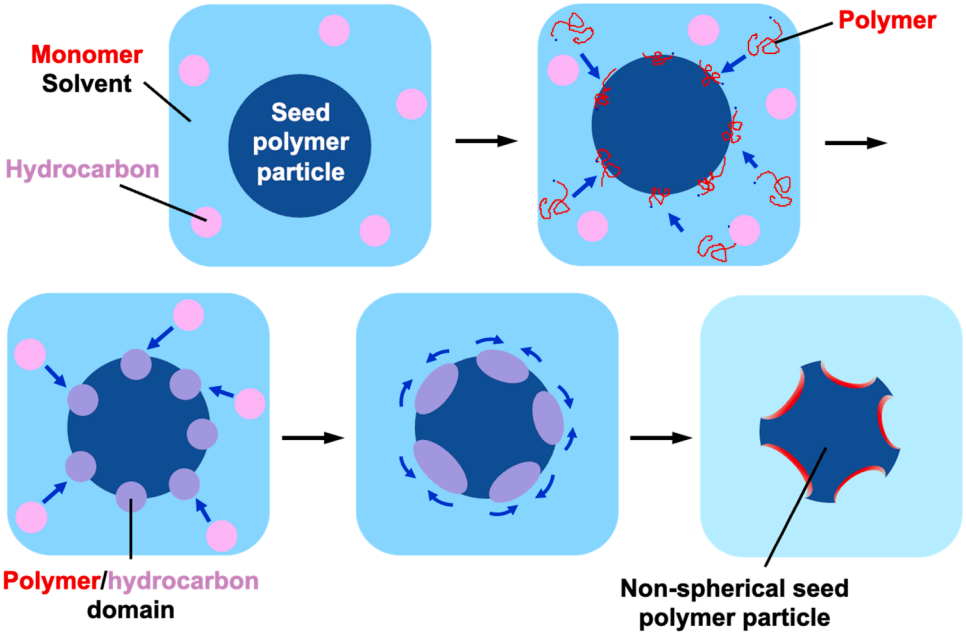

Scheme 1. Preparation of nonspherical polymer particles via SDP.

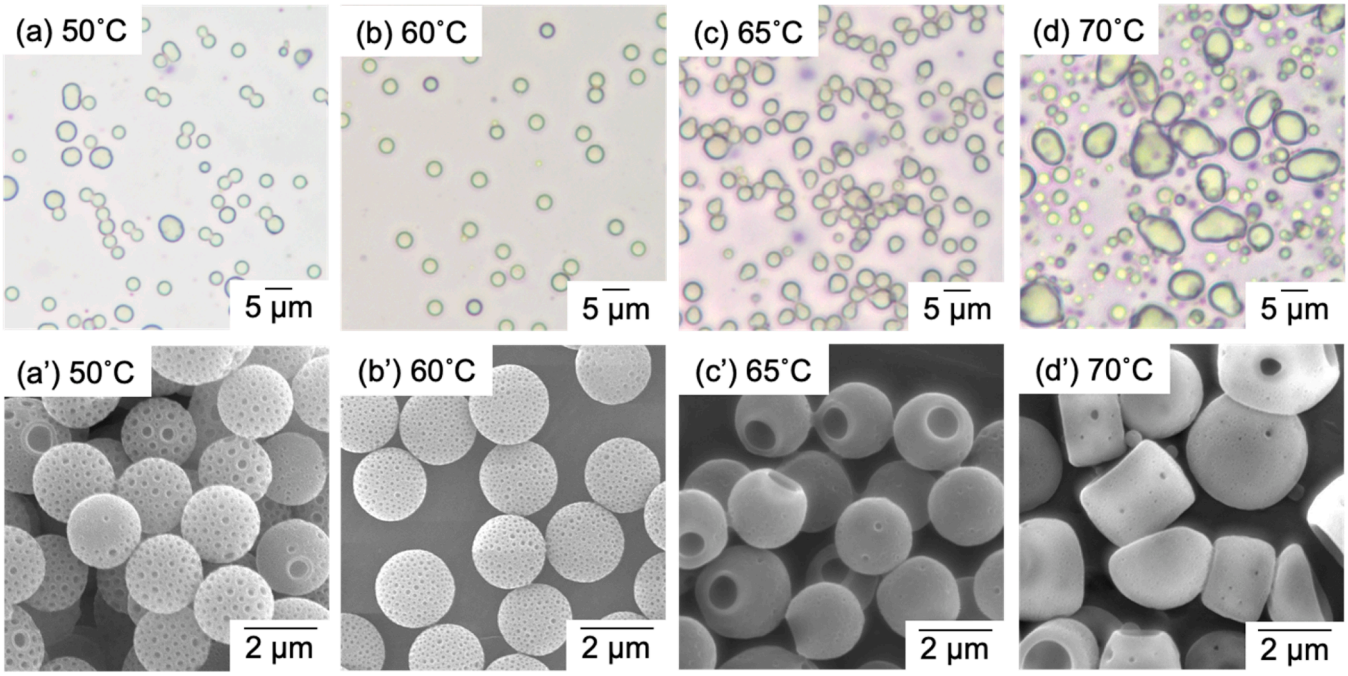

Fig. 2. Optical micrographs of PMMA–PS–decalin composite particles prepared via SDP of styrene in presence of decalin droplets at various temperatures (a–d). SEM images of PMMA–PS particles obtained after extracting decalin from composite particles using methanol (a'–d').

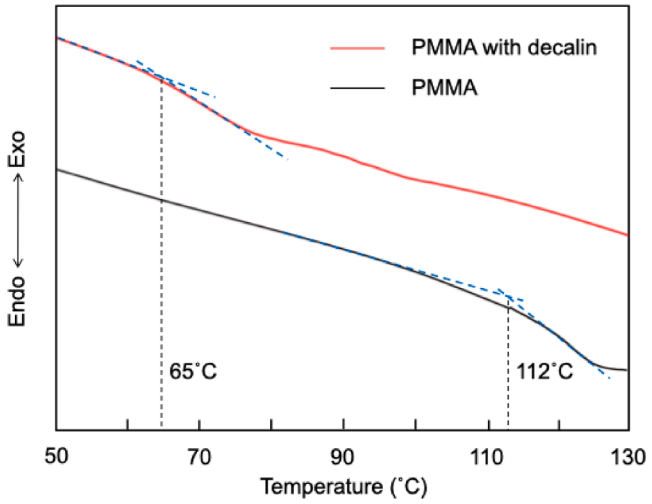

Fig. 3. DSC second-heating curves of PMMA particles with and without decalin.

the HSP distance, resulting in a T_g decrease. The T_g of PMMA in the presence of tetralin or indan was also measured via DSC as in the decalin system, resulting in T_g values with tetralin and indan at approximately 20°C and 0°C, respectively (Figure S4). Thus, indan and tetralin plasticized the PMMA particles more than decalin. Fig. 4 shows the optical microscope images of the obtained PMMA/PS–hydrocarbon composite particles and SEM and TEM images of the obtained PMMA/PS particles after washing with methanol. The optical microscope images (Figs. 4(a)–4(c)) show that the particles obtained using indan or tetralin as the hydrocarbon were more swollen than those prepared using decalin, and the domains on the composite particles were submerged. According to the SEM (Fig. 4(a')–4(c')) and TEM (Fig. 4(a'')–4(c'')) images, the particles synthesized using indan as the hydrocarbon exhibited shrinkage of the concavities during washing and drying at room temperature due to PMMA plasticization, resulting in small, bowl-like particles. In the case of tetralin, PMMA had high viscosity and maintained its shape during washing and drying, resulting in large, bowl-like particles. When using indan or tetralin, optical microscopy images revealed spherical objects (Figs. 4(a)-4(b)). However, with careful observation, a smaller inner domain was observed within the swollen particle. This inner domain was considered to be the PS phase swollen with hydrocarbon. The depression part observed in the SEM image was a void formed by the removal of hydrocarbon. Additionally, the shrinkage factor (defined as the particle diameter from SEM images divided by that from optical microscopy images) was calculated. The shrinkage factors for particles with decalin, tetralin, and indan were 0.72, 0.64, and 0.57, respectively. These results were consistent with the swelling behavior predicted from the HSP distance, suggesting that the swelling behavior of polymer particles in the presence of hydrocarbons could be estimated based on the HSP distance between the hydrocarbon and the seed polymer. Therefore, the T_r and T_g of the seed polymer ($T_{g,seed}$) were important for particle shape control during SDP.

We quantified the above results by comparing the shape change of the PMMA particles in this study with that of PS seed particles in a previous study [16] based on their T_r and T_g differences. The T_g of the PMMA seed particles ($T_{g,PMMA}$) with decalin as the hydrocarbon was 65°C. At T_r of 40°C, 50°C, 60°C, 65°C, and 70°C, the $T_r-T_{g,PMMA}$ values were −25, −15, −5, 0, and 5, respectively. The resulting particle morphologies were as follows: core–shell at $T_r-T_{g,\ PMMA}$ of −25, golf ball-like at $T_r-T_{g,PMMA}$ of −15 to −5, bowl-like at $T_r-T_{g,PMMA}$ of 0, and barrel-like at $T_r-T_{g,PMMA}$ of 5. With tetralin and indan as the hydrocarbons, the $T_{g,PMMA}$ values were 20°C and 0°C, respectively. At T_r of 65°C, the $T_r-T_{g,PMMA}$ values were 45 and 65, respectively, with bowl-like particles formed in both cases. Thus, in SDP of styrene using PMMA particles as seeds, core–shell structures formed at $T_r-T_{g,PMMA}$ of −25 or lower, golf ball-like structures formed at $T_r-T_{g,PMMA}$ of approximately −15 to around −5, and bowl- or barrel-like structures formed at $T_r-T_{g,PMMA}$ of 0 or higher. In the case of SDP of EHMA using PS particles as seeds [16], the T_g values of the PS seed particles ($T_{g,PS}$) with hexadecane, tetradecane, dodecane, and decane as hydrocarbons were 54°C, 49°C, 42°C, and 35°C, respectively. At T_r of 60°C, the corresponding $T_r-T_{g,PS}$ values were 6, 11, 18, and 25, respectively. The resulting particle morphologies were as follows: golf ball-like at $T_r-T_{g,PS}$

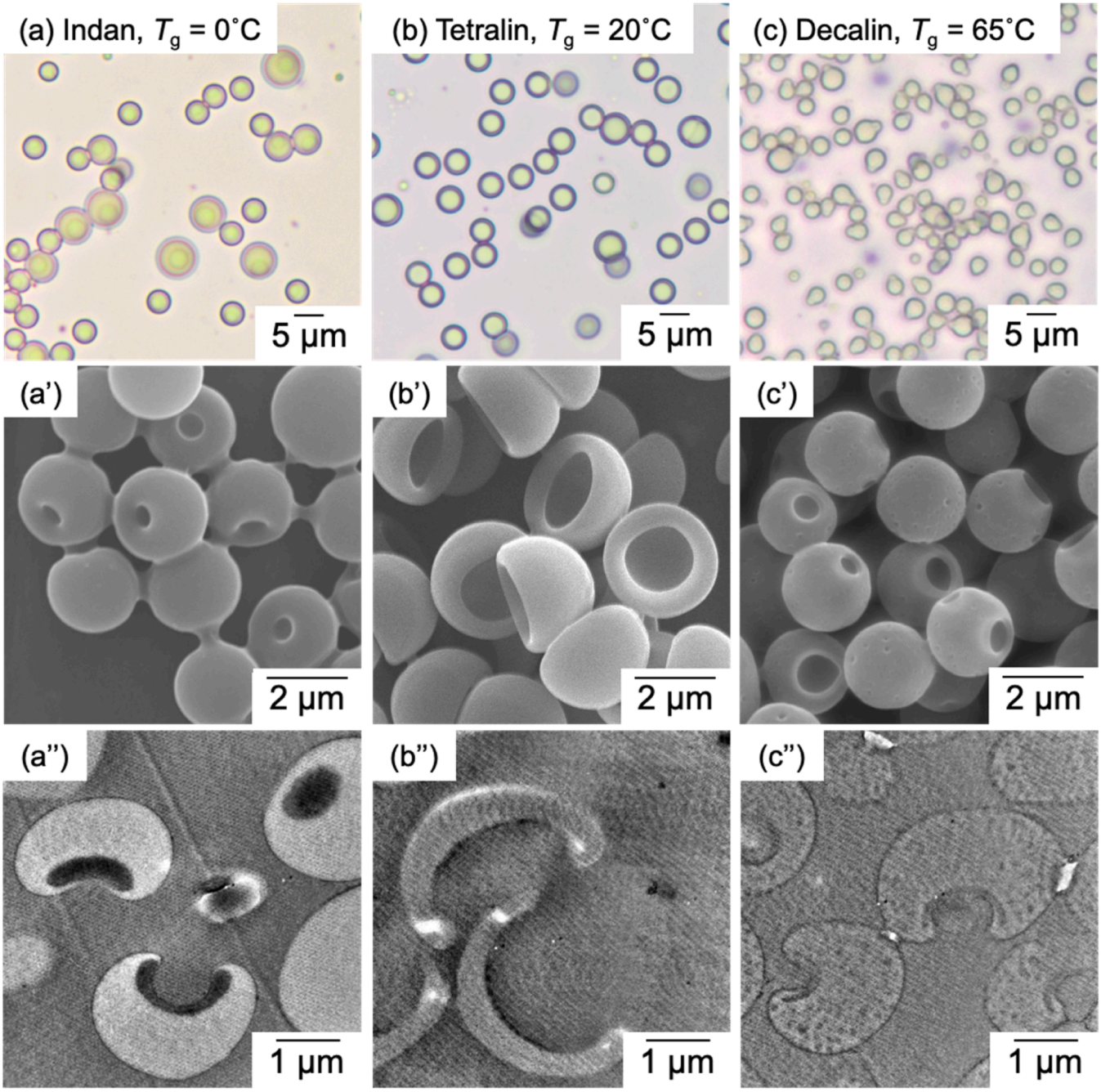

Fig. 4. Optical micrographs of PMMA–PS–hydrocarbon composite particles prepared via SDP of styrene at 65°C in presence of indan (a), tetralin (b), or decalin (c). SEM images of PMMA–PS particles obtained after extracting indan (a'), tetralin (b'), or decalin (c') from composite particles using methanol. TEM images of ultrathin cross sections of PMMA–PS particles obtained after extracting indan (a''), tetralin (b''), or decalin (c'') from composite particles using methanol.

of 6, polyhedron-like at $T_r - T_{g,PS}$ of 11–18, and disk-like at $T_r - T_{g,PS}$ of 25. Therefore, the particle deformation increased with $T_r - T_{g.seed}$.

We further studied the adsorption behavior of the domains on the seed particle by focusing on the affinity of the seed and second polymer for the medium (Table S1). The absolute difference between the HSP distance of the seed polymer to the medium and that of the second polymer to the medium was defined as H. Here, when PMMA and PS were used as the seed and second polymer, respectively, H = 2.44. However, with PS and PEHMA as the seed and second polymer, respectively, H = 0.33. The significant difference in the affinity of the seed polymer and the second polymer to the medium in the case of the PMMA seed particles caused the domains to submerge into the seed particles, resulting in bowl-like particles. Therefore, shifting H of PMMA and PS closer to 0 should suppress domain submergence.

To change the hydrophilicity of the second polymer, we conducted SDP of styrene using AIBN/VPE-0201 (1/1, w/w) as initiators, in which VPE-0201 had hydrophilic poly(ethylene glychol) segments. Fig. 5 shows optical microscope images of the obtained PMMA/PS–hydrocarbon composite particles and SEM and TEM images of the obtained PMMA/PS particles. With decalin as the hydrocarbon, slightly flattened bowl- or barrel-like particles were observed. With tetralin as the hydrocarbon, shallow bowl- or disk-like particles were obtained. Thus, the use of the hydrophilic initiator suppressed the submergence of the domains composed of the second polymer and hydrocarbons. Furthermore, the morphology of these polymer particles could be controlled by modifying the internal viscosity of the seed particle ($T_r - T_{g,seed}$) and the

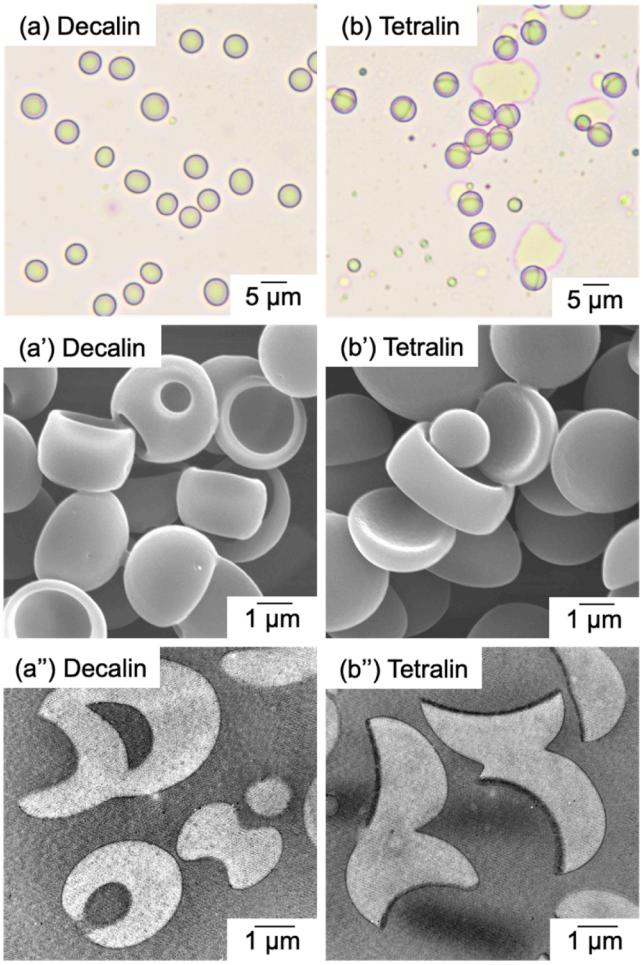

Fig. 5. Optical micrographs of PMMA–PS–hydrocarbon composite particles prepared via SDP of styrene at 65°C in presence of decalin (a) or tetralin (b) using AIBN/VPE-0201 (1/1, w/w) as initiators. SEM images of PMMA–PS particles obtained after extracting decalin (a') or tetralin (b') from composite particles using methanol. TEM images of ultrathin cross sections of PMMA–PS particles obtained after extracting decalin (a'') or tetralin (b'') from composite particles using methanol.

H value during SDP. However, the particle morphology obtained using PEG-OH instead of VPE-0201 was comparable to that obtained using only AIBN as an initiator (Figure S5(a)). This observation implied that VPE-0201 contributed to particle deformation by functioning as an initiator. Furthermore, nonspherical PMMA particles were obtained by extracting the PS phase using cyclohexane (a good solvent for PS but not for PMMA), in which the PMMA particle morphology was essentially the same as before extraction (Figure S5(b)).

4. Conclusion

We successfully produced PMMA particles with various morphologies—golf ball-like, bowl-like, barrel-like, and disk-like structures—by conducting SDP using PMMA particles as seeds; using decalin, tetralin, and indan as hydrocarbons; varying the reaction temperature; and using a highly hydrophilic initiator. Furthermore, we demonstrated the potential of predicting the degree of particle deformation based on the difference between the reaction temperature and the glass transition temperature of the seed particles in the presence of hydrocarbons. In addition, we formulated an HSP-based index to characterize particle shape transformations in SDP and validated its effectiveness. These findings contribute to the establishment of a generalized method for particle shape control in the fabrication of nonspherical polymer particles via SDP for any polymer species.

What's Next?

This study demonstrated a promising strategy for controlling the shapes of polymer particles using seeded dispersion polymerization (SDP), offering new pathways to engineer materials with specific functions. By understanding the influence of reaction temperature, material compatibility, and initiator type on particle morphology, this approach can be extended to other polymers beyond PMMA and PS. Designed particles will be applicable for specialized applications in fields such as drug delivery, sensors, and advanced coatings. Additionally, investigating how particle shape affects collective behavior and performance in functional systems could further unlock new frontiers in material science and nanotechnology.

Author contributions

All authors have approved the final version of the manuscript.

Declaration of Generative AI and AI-assisted technologies in the writing process

The authors declare no using generative AI and AI-assisted technologies in the writing process

Supporting Information

Supporting information is available free of charge at https://XXXXXXX. DSC data of PMMA particles in the presence of tetralin or indan, HSP data for various polymers and polymerization solvents.

Declaration of Competing Interest

The authors declare that they have no known competing financial interests or personal relationships that could have appeared to influence the work reported in this paper.

Acknowledgments

This work was partially supported by Grant-in-Aid for Scientific Research (Grant No. 23H02025) from the Japan Society for the Promotion of Science (JSPS).

Appendix A. Supporting information

Supplementary data associated with this article can be found in the online version at doi:10.1016/j.nxmate.2025.101432.

References

[1] J.A. Champion, Y.K. Katare, S. Mitragotri, Making polymeric micro- and nanoparticles of complex shapes, Proc. Natl. Acad. Sci. 104 (2007) 11901–11904, https://doi.org/10.1073/pnas.0705326104.
[2] Q. Niu, M.W. Pan, J.F. Yuan, X. Liu, X.M. Wang, H.F. Yu, Anisotropic nanoparticles with controllable morphologies from non-cross-linked seeded emulsion polymerization, Macromol. Rapid Commun. 34 (2013) 1363–1367, https://doi.org/10.1002/marc.201300431.
[3] M. Yang, Y.G. Guo, Q. Wu, Y. Luan, G. Wang, Synthesis and properties of amphiphilic nonspherical SPS/PS composite particles by multi-step seeded swelling polymerization, Polymer 55 (2014) 1948–1954, https://doi.org/10.1016/j.polymer.2014.02.064.
[4] R. Morimoto, T. Suzuki, H. Minami, Preparation of polypropylene-composite particles by dispersion polymerization, Langmuir 37 (2021) 10388–10393, https://doi.org/10.1021/acs.langmuir.1c01674.
[5] P.F. Noble, O.J. Cayre, R.G. Alargova, O.D. Velev, V.N. Paunov, Fabrication of "Hairy" colloidosomes with shells of polymeric microrods, J. Am. Chem. Soc. 126 (2004) 8092–8093, https://doi.org/10.1021/ja047808u.
[6] G. Wu, W. Li, W.N. Ni, L. Chen, G. Sun, B. You, Preparation of nonspherical fluorinated acrylate polymer particles by a "Surface Tension Controlling" method and their applications in light-diffusing films, Macromol. Mater. Eng. 304 (2019), https://doi.org/10.1002/mame.201900174.

[7] C.H. Chen, X.F. Li, J. Deng, Z. Wang, Y. Wang, Shape engineering of biomass-derived nanoparticles from hollow spheres to bowls through solvent-induced buckling, Chemsuschem 11 (2018) 2540–2546, https://doi.org/10.1002/cssc.201801215.
[8] D.H. Kim, H.C. Woo, M.H. Kim, Room-temperature synthesis of hollow polymer microparticles with an open hole on the surface and their application, Langmuir 35 (2019) 13700–13710, https://doi.org/10.1021/acs.langmuir.9b02780.
[9] D.H. Kim, J.H. Jeong, H.-C. Woo, M.H. Kim, Synthesis of highly porous polymer microspheres with interconnected open pores for catalytic microreactors, Chem. Eng. J. 420 (2021) 127628, https://doi.org/10.1016/j.cej.2020.127628.
[10] B. Yu, H.L. Cong, Q.H. Peng, C.T. Gu, Q. Tang, X.D. Xu, C. Tian, F. Zhai, Current status and future developments in preparation and application of nonspherical polymer particles, Adv. Colloid Interface Sci. 256 (2018) 126–151, https://doi.org/10.1016/j.cis.2018.04.010.
[11] Y. Liu, G.H. Li, Y.J. Zhang, L. Zhang, Hydrodynamics of irregular-shaped graphite particles in coaxial two-phase jet flow, ACS Omega 6 (2021) 16631–16640, https://doi.org/10.1021/acsomega.1c02053.
[12] D. Dendukuri, K. Tsoi, T.A. Hatton, P.S. Doyle, Controlled synthesis of nonspherical microparticles using microfluidics, Langmuir 21 (2005) 2113–2116, https://doi.org/10.1021/la047368k.
[13] W. Li, T. Suzuki, H. Minami, A facile method for preparation of polymer particles having a "Cylindrical" shape, Angew. Chem. Int. Ed. 57 (2018) 9936–9940, https://doi.org/10.1002/anie.201805700.
[14] W. Li, T. Suzuki, H. Minami, The interface adsorption behavior in a pickering emulsion stabilized by cylindrical polystyrene particles, J. Colloid Interface Sci. 552 (2019) 230–235, https://doi.org/10.1016/j.jcis.2019.05.058.
[15] M. Onishi, Y. Tsujishita, W. Li, T. Suzuki, H. Minami, Preparation of cylindrical janus particles using a stirring method, ACS Omega 5 (2020) 33047–33052, https://doi.org/10.1021/acsomega.0c04538.
[16] T. Fujibayashi, M. Okubo, Preparation and thermodynamic stability of micron-sized, monodisperse composite polymer particles of disc-like shapes by seeded dispersion polymerization, Langmuir 23 (2007) 7958–7962, https://doi.org/10.1021/la7007842.
[17] T. Fujibayashi, T. Tanaka, H. Minami, M. Okubo, Thermodynamic and kinetic considerations on the morphological stability of “Hamburger-like” composite polymer particles prepared by seeded dispersion polymerization, Colloid Polym. Sci. 288 (2010) 879–886, https://doi.org/10.1007/s00396-010-2211-0.
[18] S.Y. Qiao, S.S. Li, Q. Song, B. Liu, Shape-tunable biconcave disc-like polymer particles by swelling-induced phase separation of seeded particles with hydrophilic shells, Langmuir 39 (2023) 1190–1197, https://doi.org/10.1021/acs.langmuir.2c02995.
[19] M. Okubo, R. Takekoh, A. Suzuki, Preparation of micron-sized, monodisperse Poly (methyl methacrylate)/polystyrene composite particles having a large number of dents on their surfaces by seeded dispersion polymerization in the presence of decalin, Colloid Polym. Sci. 280 (2002) 1057–1061, https://doi.org/10.1007/s00396-002-0661-8.
[20] N. Rajabalinia, S. Hamzehlou, J.R. Leiza, J.M. Asua, Experimental validation of a mathematical model for the evolution of the particle morphology of waterborne polymer-polymer hybrids: paving the way to the design and implementation of optimal polymerization strategies, Chem. Eng. J. 363 (2019) 259–269, https://doi.org/10.1016/j.cej.2019.01.140.
[21] N. Rajabalinia, S. Hamzehlou, E. Modin, A. Chuvilin, J.R. Leiza, J.M. Asua, Coupling HAADF-STEM tomography and image reconstruction for the precise characterization of particle morphology of composite polymer latexes, Macromolecules 52 (2019) 5298–5306, https://doi.org/10.1021/acs.macromol.9b00787.
[22] T. Morishita, I. Maitani, T. Michiura, N. Suzuki, T. Suzuki, K. Akamatsu, H. Minami, Preparation of golf ball-like polymer particles bearing site-selective functional groups, ACS Appl. Mater. Interfaces 16 (2024) 64058–64064, https://doi.org/10.1021/acsami.4c15686.